Electronic Supplementary Material (ESI) for ChemComm.

Supporting Information

Two-photon fluorescence self-reporting black phosphorus nanoprobe for in situ monitoring therapy response

Kesong Guan[#a], Peng Wang[#a], Fang Zhou[a], Youjuan Wang[a], Hong-Wen Liu[a], Qingji Xie[b], Guosheng Song[a], Xia Yin[*a], Shuangyan Huan[*a] and Xiao-Bing Zhang[a]

[a.] *State Key Laboratory of Chemo/Biosensing and Chemometrics, College of Chemistry and Chemical Engineering, Hunan University, Changsha, Hunan 410082, P. R. China.*

[b.] *Key Laboratory of Chemical Biology and Traditional Chinese Medicine, Hunan Normal University, Changsha, Hunan 410081, P. R. China.*

Experimental Section

Materials and instrumentation. All chemicals were purchased from commercial reagent companies and were used without any purification. Ultrapure water (resistance > 18 $M\Omega \cdot cm^{-1}$) was taken from the Milli-Q reference system (Millipore). Dynamic Light Scattering (DLS) measurements were performed using a Zeta sizer 3000Hs (Malvern). Fluorescent signals were recorded using a Fluoromax-4 spectrofluorometer (HORIBA Jobin Yvon). The UV absorption spectrum was recorded using a UV-2450 UV-vis spectrometer (Shimadzu). Single-photon and two-photon-excited cell and tissue imaging using the FV1000-MPE multiphoton laser scanning confocal microscope (Olympus).

Synthesis of BPNS. The BPNS were prepared by the liquid exfoliation of corresponding bulk black phosphorus sample. Briefly, 20 mg of the bulk black phosphorus was added to 40 mL of ultrapure water, then was bubbled with argon to eliminate dissolved oxygen molecules during the exfoliation process. Next, the mixture solution was sonicated in ice water for 12 h (Amplifier: 25%, On/Off cycle: 45 s/15 s). The obtained brown dispersion was centrifuged at 1000 rpm for 10 min to get rid of unexfoliated bulk black phosphorus. Then, the supernatant containing BPNS was collected and purified by Amicon tubes (MWCO 100kDa; Millipore). The resulted pure BPNS was stored in PBS under 4 °C for further use.

Synthesis of compound A-Br: Compound A-OH (1.500 g, 7.2 mmol) and anhydrous toluene (40 mL) were added into a two-necked round bottom flask, and then the mixed solution was cooled to 0 ° C in an ice bath and nitrogen atmosphere, and then phosphorus tribromide (PBr_3, 0.8 mL, 8.51 mmol) was added dropwise. The mixed solution was reacted at 0 ° C for 1 h. After returning to room temperature, the reaction solution was slowly added with the saturated Na_2CO_3 solution (15 mL), until the solution became neutral or weakly acidic. Finally, the product was separated from toluene, extracted with water and brine, dried with anhydrous Na_2SO_4, and concentrated to afford compound A-Br (1.769 g, 91%).

Synthesis of compound 2: Compound 1 (4-bromo-1, 8-naphthalic anhydride,

0.276 g, 1 mmol) and NaN_3 (0.195 g, 3 mmol) were dissolved in N, N-dimethylformamide (DMF) / H_2O (v/v, 10/1, 20 mL) and stirred at 80 °C for 2 h. Then, the solvent was poured into ice water (10 ml), and the precipitated solid was filtered. Subsequently, the solid was dissolved in DMF (20 ml), added with 2ml of H_2O containing NaHS (0.224 g, 4 mmol) and stirred at 90 °C for 2h. Next, the reaction solution was added with ice water and adjusted to weak acidity. Finally, the yellow solid precipitated was collected and filtered to afford compound 2 (0.18 g, 81%).

Synthesis of compound 3: Compound 3 was synthesized according to previous work.[1] Compound 2 (0.107 g, 0.5 mmol), compound A-Br (0.135 g, 0.5 mmol) and K_2CO_3 (0.138 g, 1 mmol) were dissolved in DMF and stirred at 90 °C for 1 h. Then, the solvent was evaporated in vacuo. The residue was purified by the silica gel chromatography using CH_2Cl_2/CH_3OH (10:1, v/v) as the mobile phase to afford compound 3 as yellow solid (0.153 g, 76%).

Synthesis of MNAC: 4-aminobutanoic acid (0.154 g, 1.5 mmol) and compound 3 (0.142 g, 0.35 mmol) were dissolved in C_2H_5OH (20 mL) and stirred at 86 °C overnight. The solvent was evaporated in vacuo to remove ethanol, and then the residue was added with water to let the solid crude product precipitation. After filtration, the product was collected and extracted with CH_2Cl_2. Next, CH_2Cl_2 was evaporated in vacuo to afford crude solid, which was further purified by column chromatography on silica gel using CH_2Cl_2/CH_3OH (5:1, v/v) to gain product MNAC (0.081 g, 48%). ^{1}H NMR (DMSO-d_6, 400 MHz), δ(ppm): δ 8.73 (d, J = 4.0 Hz, 2H), δ 8.43 (d, J = 8.0 Hz, 2H), δ 8.35 (d, J = 4.0 Hz, 2H), δ 8.21(d, J = 8.0 Hz, 2H), δ 7.96 (s, 1H), δ 7.57 (m, 5H), δ 7.32 (d, J = 8.0 Hz, 2H), δ 5.49 (s, 2H), δ 4.11 (t, J = 6.0 Hz, 2H), δ 2.31 (t, J = 8.0 Hz, 2H), δ 1.91(m, 2H). ^{13}C NMR (DMSO-d_6, 400 MHz), δ 23.84, 32.13, 105.06, 108.89, 120.69, 122.24, 124.64, 125.66, 128.30, 131.09, 134.68, 151.06, 163.57, 164.37, 174.57. ESI-MS (m/z): $C_{31}H_{24}N_2O_4$, found 485.34.

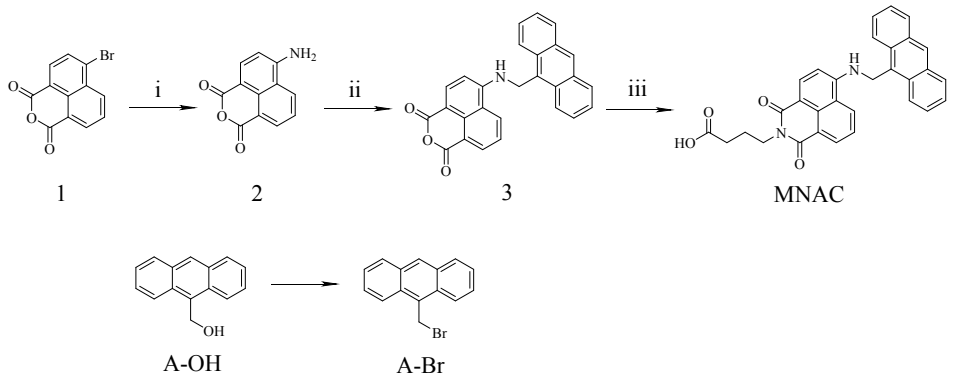

Scheme.1 Synthesis route of fluorescent probe MNAC.

Synthesis of TPBP. **TPBP** is composed of BPNS with MNAC and NH_2-PEG_{2000}-NH_2 linker. First, the as-prepared BPNS (1 mg) was dispersed into deoxygenated ultrapure water (1 mL), then added with NH_2-PEG_{2000}-NH_2 (10 mg). After ultrasonication for 30 minutes, the mixture was stirred at room temperature for 4 h. The obtained PEG loaded BPNS were gathered by Amicon tubes (MWCO 100kDa; Millipore) and washed in ultrapure water to remove excessive PEG. Then, the mixture was added with MNAC (1 mg), 1-(3-dimethylaminopropyl)-3-ethylcarbodiimide hydrochloride (EDC·HCl, 2 mg) and N-hydroxyamber imide (NHS, 2 mg), and stirred at room temperature overnight. The final product **TPBP** were obtained through Amicon tubes (MWCO 100kDa; Millipore) and rinsing for another three times to remove the remaining unreacted materials.

Photodynamic activity test of TPBP. 5 mL of 1, 3-diphenylisobenzofuran (DPBF) solution (20 μg·mL^{-1}) in DMSO was mixed with BPNS (10 μg·ml^{-1}) or **TPBP** (35 μg·mL^{-1}) solution and stirred in dark for 2 h. The sample was irradiated by laser (660 nm, 0.1 W·cm^{-2}), then measured by UV-vis absorption spectra at different time points, and pure water with DPBF was employed as control.

Self-reporting photodynamic test of TPBP. TPBP solution (1 mL, 50 μg·mL^{-1}), was irradiated with a 660 nm light (0.5 W·cm^{-2}), and the fluorescence signal changes of **TPBP** at different time periods were recorded. The excitation wavelength is 440 nm. MNAC solution without BPNS was used as a control experiment.

Cell culture assays and in vitro toxicity study. HeLa and 4T1 cells were

purchased from ATCC (American Type Culture Collection, Manassas, VA, USA). HeLa cells were cultured in DMEM (Dulbecco's modified Eagle medium) or 4T1 cells were cultured in RPMI-1640 culture medium, supplemented with 10% FBS (fetal bovine serum, GIBCO) and antibiotics (10 U/mL penicillin and 10 mg/mL streptomycin) in a humidified environment at 37 ºC in 5% CO_2 atmosphere. HeLa cells were seeded at a density of 5000 cells/well in 96-well plates and incubated overnight. Then, the cells were incubated with **TPBP** at different concentration (0, 5, 10, 20, 50, 100, 200 $\mu g \cdot ml^{-1}$) for 24 h. Five multiple holes were set for every concentration. The formulations were changed with 3-(4, 5-dimethyl-2-thiazolyl)-2, 5-diphenyl-2-H-tetrazolium bromide (MTT) contained DMEM (5 $mg \cdot mL^{-1}$). A microplate reader was used to measure the absorbance at 490nm.

Self-reported PDT of TPBP in vitro. HeLa cells were planted in 96-well plates at a density of 5×10^3 per well and incubated for 24 h. Then, the culture medium in each well was replaced with **TPBP** (25 $\mu g \cdot mL^{-1}$) in the culture medium. After being cultured for 4 h, the cells in PDT group were irradiated with 660 nm laser (0.5 $W \cdot cm^{-2}$) for 10 min. Next, the cells were cultured at 37 °C for 24 h. The cytotoxicity of **TPBP** was determined by standard MTT assay. To verify the ability of self-reporting of **TPBP** in vitro, HeLa cells were seeded at a density of 5 x 10^3 cells per well into 96-well plates for 24 h and then incubated with **TPBP** (25 $\mu g \cdot mL^{-1}$) for additional 4 h. After different time periods (0, 2, 4, 6, 8, 10 min) irradiation, fluorescence images were collected by the IVIS Lumina XR Imaging (Caliper, USA) imaging system. Then, those cells were further incubated for 24 h. The cytotoxicity was determined by standard MTT assay.

In vivo biosafety and antitumor efficiency of TPBP. Female BALB/c mice were purchased from Hunan SLAC Laboratory Animal Co. Ltd. and all live animal operations were in accord with institutional animal use and care regulations, according to protocol No. SYXK (Xiang) 2018-0006, approved by Animal Ethics Committee of College of Biology (Hunan University). The tumor model was generated by subcutaneously injecting saline containing 2×10^6 4T1 cells into the back of each mouse. All the mice were randomly divided into six groups (6 mice in each

group) and received the following treatment: (I) Saline (50 μL); (II) 15 min of laser irradiation; (III) **TPBP** (50 μL, 0.5 mg·kg^{-1}) only; (IV) **TPBP** (50 μL, 0.5 mg·kg^{-1}) + 5 min of laser irradiation; (V) **TPBP** (50 μL, 0.5 mg·kg^{-1}) + 10 min of laser irradiation; (VI) **TPBP** (50 μL, 0.5 mg·kg^{-1}) + 15 min of laser irradiation, respectively. 2.5 h after injection, those mice received the radiation of 660 nm laser (0.5 W·cm^{-2}) for different time. The tumor volume was calculated according to the following formula: tumor volume (mm^3) = 1/2 × length × width^2. The tumor inhibition rate was calculated by following equation: tumor inhibition rate = (V_C - V_T) / V_C × 100%, where V_T is the tumor volume after the treatments, and V_C is the tumor volume of the control group.

Histological Studies. Those mice were sacrificed after 16 days of treatment. The hearts, livers, spleens, lungs, and kidneys were fixed in 4% paraformaldehyde, and then paraffin embedded sectioning was conducted for hematoxylin and eosin (H&E) staining under standard protocols. The slices were examined using a Nikon ECLIPSE 80i microscope (Nikon Instruments Inc., NY, USA).

Reference

1. H. W. Liu, S. Xu, P. Wang, X. X. Hu, J. Zhang, L. Yuan, X. B. Zhang and W. Tan, *Chem. Commun.*, 2016, **52**, 12330.

Supplemental Figures

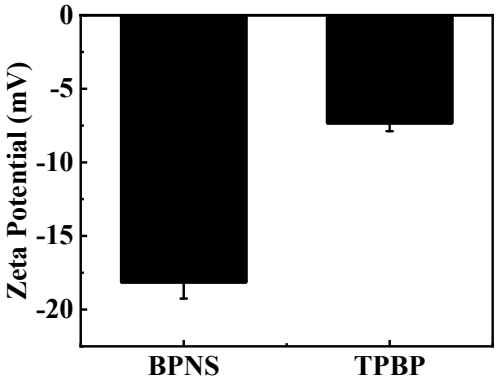

Figure S1. Zeta potential of BPNS and **TPBP** (n = 3, mean ± SD).

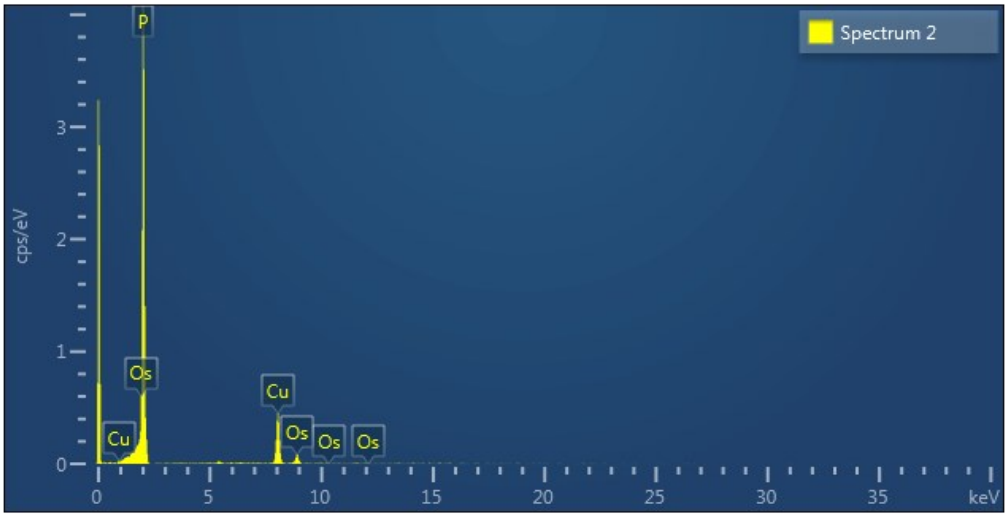

Figure S2. EDS image of **TPBP.**

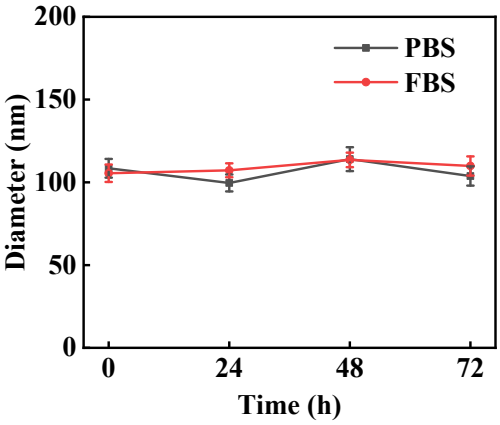

Figure S3. Stability of **TPBP** in PBS and in DMEM medium containing 10% fetal bovine serum (FBS), by monitoring particle diameter over 72 hours (n = 3, mean ± SD).

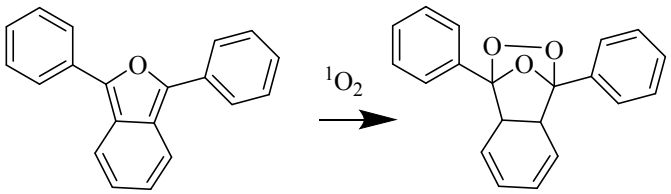

DPBF **DPBF endoperoxide**

Figure S4. $^1O_2$ detection mechanism of DPBF.

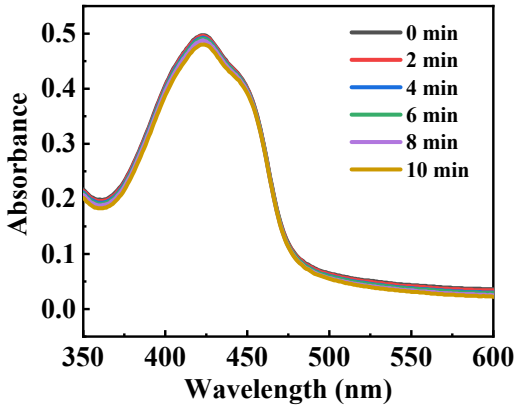

Figure S5. Detection of $^1O_2$ generation using DPBF as a probe. Time-dependent absorption spectra of DPBF in water under 660 nm laser irradiation.

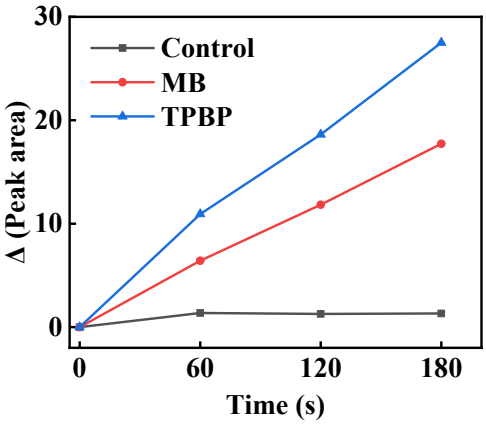

Figure S6. Time-dependent generation efficiency of $^1O_2$ from MB and **TPBP**. In details, $\Phi_{TPBP} = \Phi_{MB}$ (I_{TPBP} / I_{MB}), where I_{TPBP} and I_{MB} mean the decreased absorption peak areas of DPBF, respectively. The results show the $^1O_2$ quantum yield of **TPBP** (Φ_{TPBP}) is 0.83.

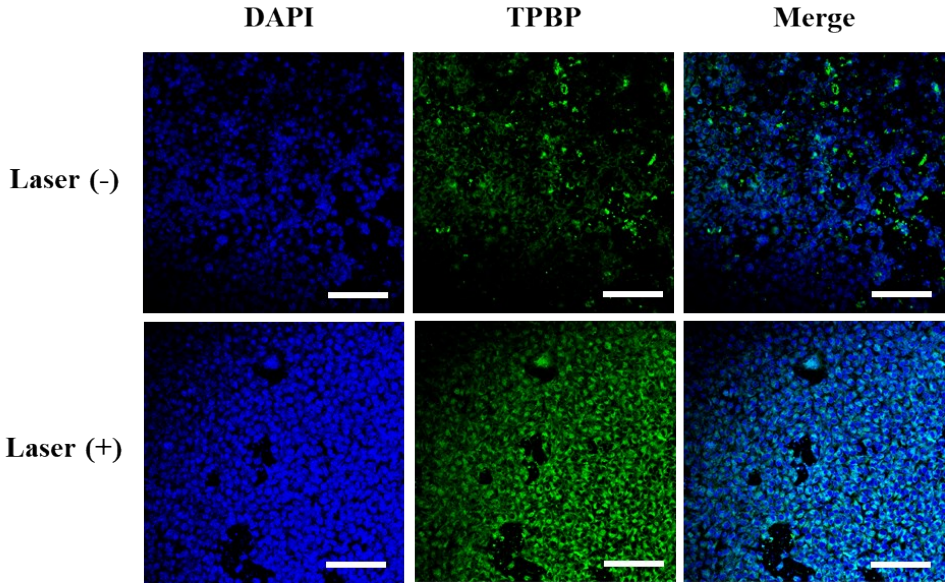

Figure S7. Confocal images of HeLa cells incubated with **TPBP** before (top row) and after (bottom row) 660 nm laser irradiation (0.5 $W \cdot cm^{-2}$, 5 min). (Scale bar = 100 μm).

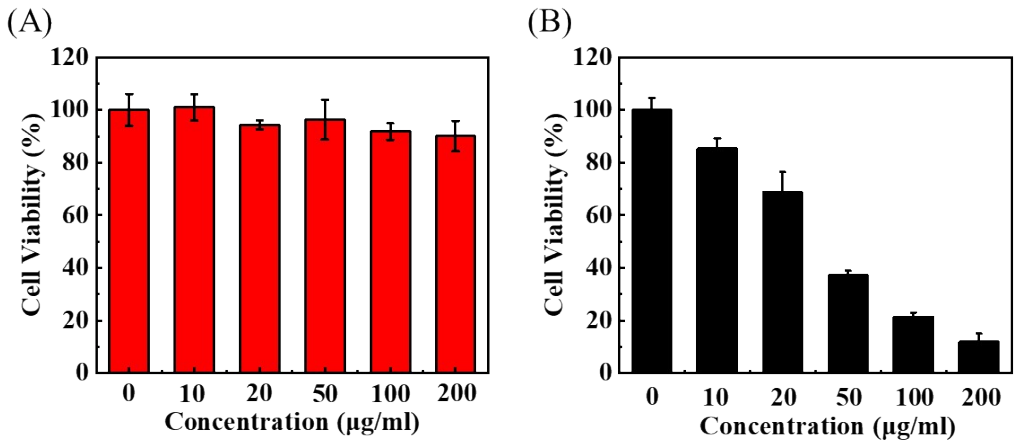

Figure S8. Cell viabilities of 4T1 cells after incubation with various concentrations (0, 10, 20, 50, 100, 200 μg/ml) of **TPBP** (A) without 660 nm irradiation and (B) with irradiation (n = 5, mean ± SD).

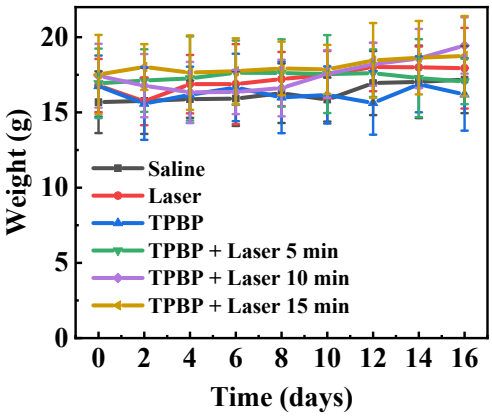

Figure S9. Body weight of mice taken every other day after various treatment with (i) saline, (ii) only Laser, (iii) only **TPBP**, (iv) **TPBP** + Laser 5 min, (v) **TPBP** + Laser 10 min, (vi) **TPBP** + Laser 15 min (n = 3, mean ± SD).

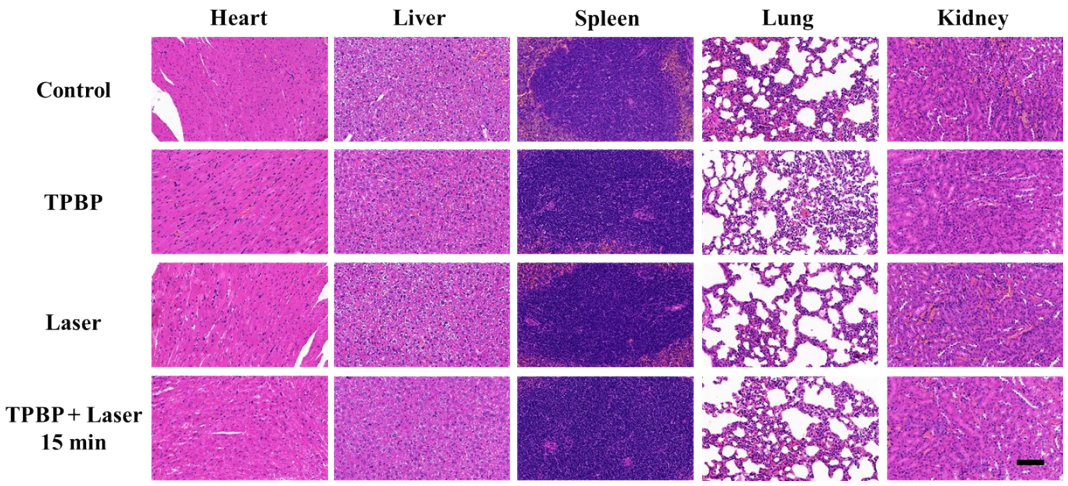

Figure S10. H&E staining of heart, liver, spleen, lung, and kidney tissue slices for different groups after treatment (on day 14): (i) Saline (control), (ii) only **TPBP**, (iii) only laser, (iv) **TPBP** + laser 15 min. (Scale bar = 50 μm)

Mass spectra and NMR data

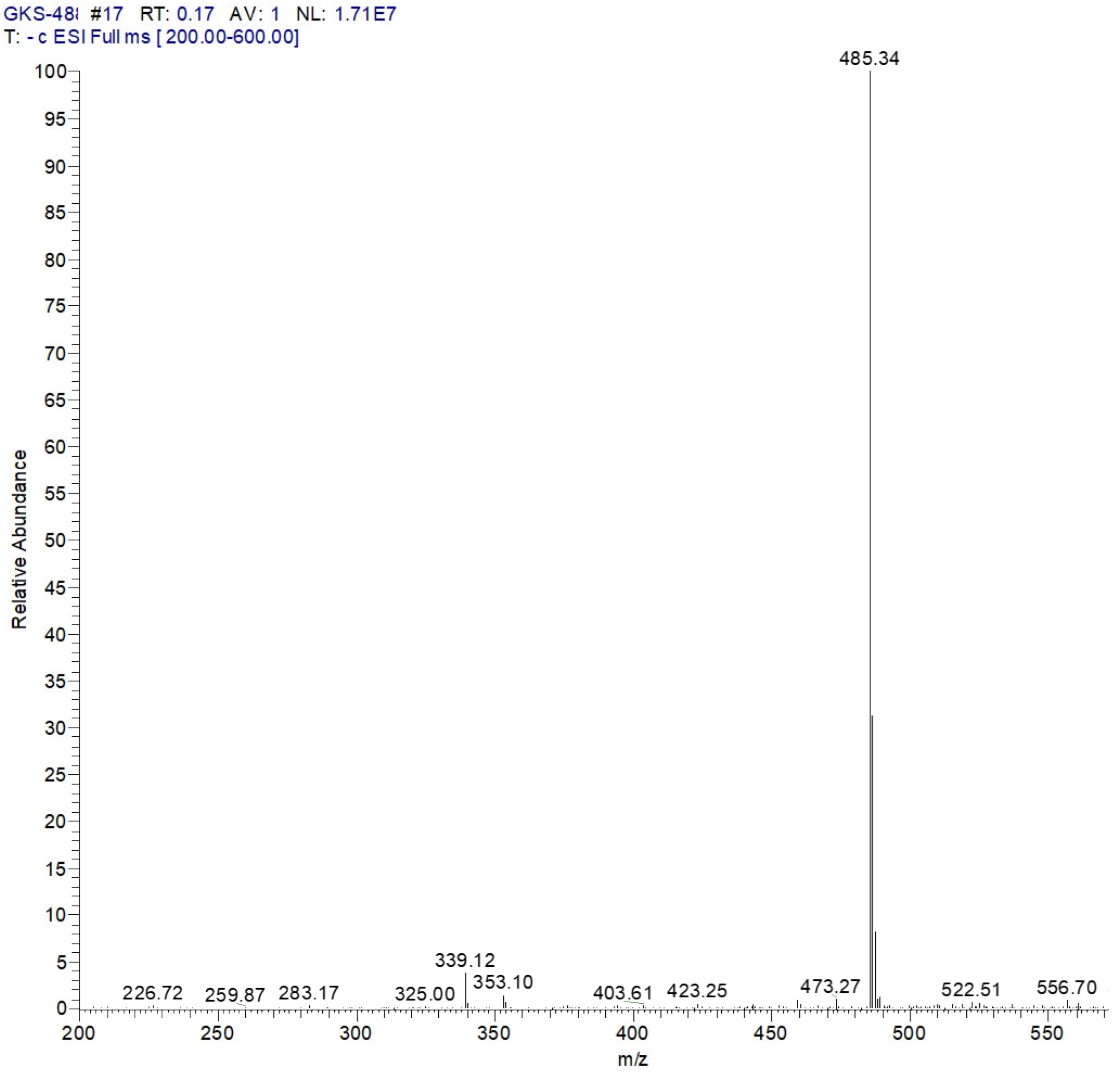

Figure S11. ESI-MS spectrum of MNAC.

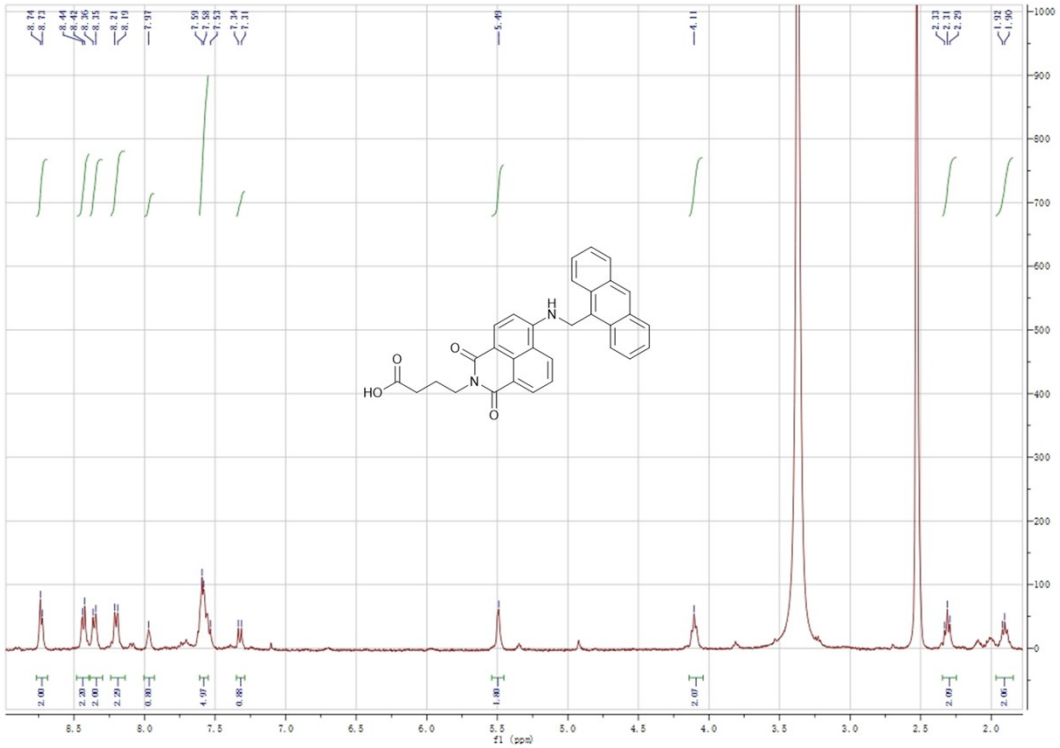

Figure S12. ^{1}H NMR spectrum of MNAC.

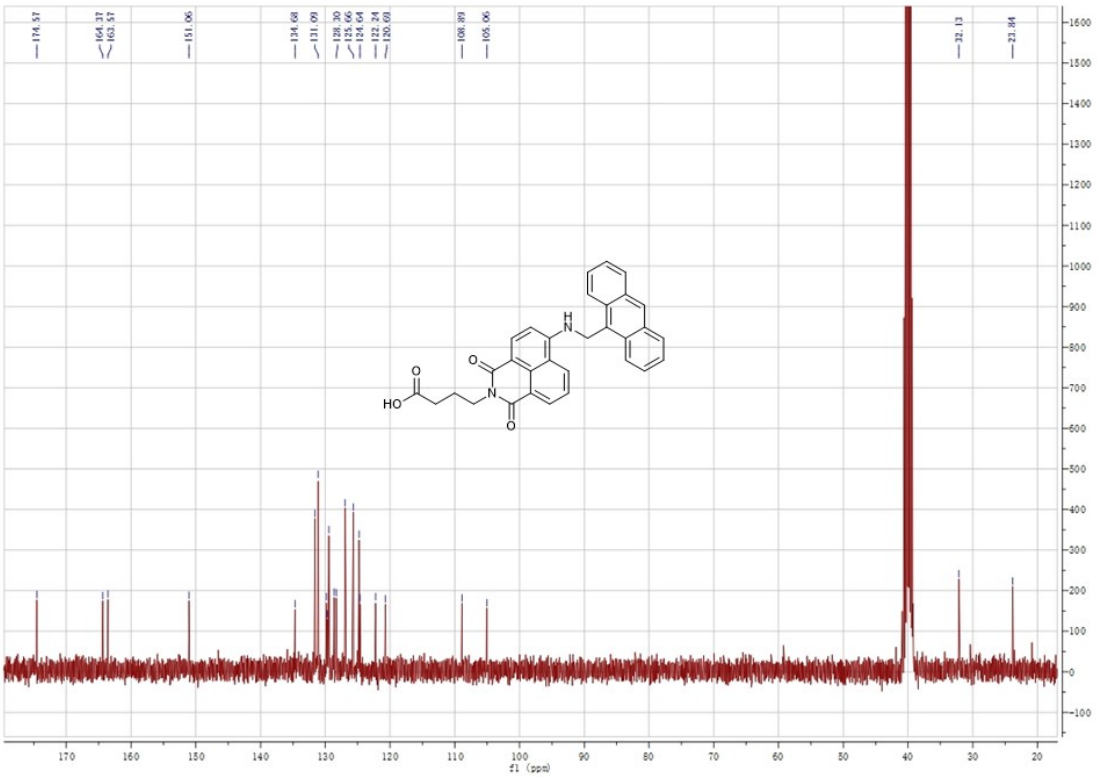

Figure S13. ^{13}C NMR spectrum of MNAC.